Direct Demonstration of Instabilities in Oxygen Concentrations within the Extravascular Compartment of an Experimental Tumor

Jennifer Lanzen,[1] Rod D. Braun,[4] Bruce Klitzman,[2,3] David Brizel,[1] Timothy W. Secomb,[5] and Mark W. Dewhirst[1,2]

Departments of [1]Radiation Oncology, [2]Biomedical Engineering, and [3]Kenan Plastic Surgery Research Labs and Biomedical Engineering, Duke University Medical Center, Durham, North Carolina; [4]Department of Anatomy and Cell Biology, Wayne State University School of Medicine, Detroit Michigan; and [5]Department of Physiology, University of Arizona, Tucson, Arizona

Abstract

To test the hypothesis that temporal variations in microvessel red cell flux cause unstable oxygen levels in tumor interstitium, extravascular oxygenation of R3230Ac mammary tumors grown in skin-fold window chambers was measured using recessed tip polarographic microelectrodes. Red cell fluxes in microvessels surrounding pO_2 measurement locations were measured using fluorescently labeled red cells. Temporal pO_2 instability was observed in all experiments. Median pO_2 was inversely related to radial distance from microvessels. Transient fluctuations above and below 10 mm Hg were consistently seen, except in one experiment near the oxygen diffusion distance limit (140 μm) where pO_2 fluctuations were <2 mm Hg and median pO_2 was <5 mm Hg. Vascular stasis was not seen in these experiments. These results show that fluctuations in red cell flux, as opposed to vascular stasis, can cause temporal variations in pO_2 that extend from perivascular regions to the maximum oxygen diffusion distance. (Cancer Res 2006; 66(4): 2219-23)

Introduction

Tumor hypoxia has classically been categorized as developing in two different forms: "chronic" and "acute." Chronic hypoxia has been attributed to large diffusion distances between tumor microvessels whereas acute hypoxia has been thought to be the result of transient vascular occlusion (1–4). We and others have argued that this categorization misleadingly implies that two independent mechanisms are responsible for hypoxia (5–7). Tumor hypoxia develops because oxygen demand exceeds supply (8–10). Causes of supply deficiency include abnormal vascular geometry (8), relatively low vascular density as compared with most normal tissues (11), and relative paucity of arteriolar supply vessels (12). These features of tumor vasculature contribute to exaggerated longitudinal vascular oxygen gradients, leading to hypoxia within some microvessels (13–15). Previously, we showed that temporal variations in microvessel red cell flux cause variations in perivascular pO_2 (16). Using theoretical simulations, we predicted that the temporal flux variations would also cause fluctuations in pO_2 throughout the subtended tissue region with a substantial fraction of tissue exhibiting transient episodes of hypoxia. In this study, we conducted experiments to test this prediction.

Requests for reprints: Mark W. Dewhirst, Research Drive, Room 201 MSRB, Box 3455 DUMC, Durham, NC 27710. Phone: 919-684-4180; Fax: 919-684-8718; E-mail: dewhirst@radonc.duke.edu.

©2006 American Association for Cancer Research.

doi:10.1158/0008-5472.CAN-03-2958

Materials and Methods

The protocol was approved by the Duke University Animal Care and Use Committee. R3230Ac mammary carcinoma cells were transplanted into dorsal skin-fold window chambers of female Fischer 344 rats as previously described (17). Circular 1-cm diameter segments of epidermis were removed from opposing surfaces of the skin flap, leaving one to two fascial layers, containing s.c. vasculature. The two halves of an anodized aluminum chamber were sutured to this tissue such that the dissected circular fascial layer was contained within the window portion of the chamber. R3230Ac tumor fragments of ~0.1-mm diameter, obtained from a donor animal, were placed onto one side of the fascial layer. The two surfaces were then covered with glass coverslips. Tumors were allowed to grow until they reached a diameter of 2 to 3 mm, which typically required 7 to 9 days. During the period of tumor growth, animals were housed individually in an environmental chamber maintained at a temperature of 34°C and 50% humidity.

Recessed, gold-plated cathode tip oxygen microelectrodes (tip diameters of 6-10 μm) were manufactured according to the method of Linsenmeier and Yancey (18). Electrodes were calibrated before and after each experiment in saline bubbled with gas mixtures of 0%, 5%, 15%, and 21% O_2.

Experiments in which calibrations drifted >20% from pre- to post-measurement time points were not used. All electrodes showed linear relationships between current generated and pO_2 with an average sensitivity of 2.99 ± 1.31 pA/mm Hg. Current was measured using a Chemical Microsensor (model 1201, Diamond General Development Corp., Ann Arbor, MI).

Erythrocytes were fluorescently labeled with DiI using the method of Unthank et al. (19). DiI was dissolved in ethanol to a concentration of 0.5 mg/mL. Blood from an anesthetized donor rat was withdrawn via cardiac puncture and the erythrocytes were isolated by centrifugation and washed in PBS. One hundred microliters of packed erythrocytes were suspended in 10 mL of PBS and 100 μL of DiI solution were added. The suspension was incubated at room temperature for 30 minutes. The labeled cells were removed from the DiI-containing solution by washing with PBS and additional centrifugation. Cells were kept in the dark once DiI was added to prevent photobleaching.

Videomicroscopy of the window chamber was used to measure red cell fluxes and to place microelectrodes to measure interstitial pO_2. A Zeiss intravital microscope workstation (Zeiss Axioskop, New York, NY) equipped with optics for transillumination and fluorescence microscopy was used to visualize the microvasculature and labeled erythrocytes during experiments. For transillumination, images were obtained using a CCD video camera (MTI CCD-72, Dage MTI, Michigan City, IN). For epifluorescence, a silicon-intensified tube camera was used (model C2400-08, Hamamatsu Photonics, Hamamatsu City, Japan). Images were recorded onto SVHS videotape (SVO-9500MD Sony Corporation of America, San Jose, CA) for later assessment of red cell fluxes.

Liposomes of 100-nm average diameter were prepared (16) for use as a fluorescent blood pool marker to assist in identifying vascular networks. The liposomes contained polyethylene glycol in the membrane to extend circulation time. The composition was hydrogenated soy

Downloaded from cancerres.aacrjournals.org on September 20, 2020. © 2006 American Association for Cancer Research.

phosphatidylethanolamine/cholesterol/polyethylene glycol (2000 M)–derivatized phosphatidylethanolamine in a molar ratio of 60:40:2.4:0.48. Lipids were purchased from Avanti Polar Lipids (Alabaster, AL).

Animals were anesthetized with pentobarbital sodium at a dose of 40 to 50 mg/kg and a femoral artery and vein were catheterized for monitoring of blood pressure and i.v. access, respectively. The animals were placed in lateral recumbency onto a temperature-controlled heating pad that was mounted on the microscope stage. Fluorescently labeled red cells were administered i.v. at a concentration to yield ~1% labeled fraction. Blood pressure and heart rate were measured using digital signals acquired from a blood pressure transducer and recorded to a PC (CODAS Micro Software, Akron, OH). A tracing of all blood vessels containing labeled liposomes was made from the video monitor.

The glass coverslip was removed and a suffusion medium (Earle's balanced salt solution) bubbled with 95% air and 5% CO_2 at 34°C (normal skin temperature) was set to flow across the window at a rate of ~1 mL/min. A silver-chloride anode was sewn into a s.c. pocket into the hind limb of the rat. A recessed-tip glass microelectrode was placed into a stage-mounted micromanipulator (Model M0102E, Narishige, Inc., Narishige, Japan) and inserted into the medium just beneath the surface. Readings represented an *in vivo* measurement equivalent to air (21% O_2). The suffusion medium was replaced with the same medium, but in this case bubbled with 95% N_2 and 5% CO_2. A tent made of Saran Wrap (Dow Brands, Indianapolis, IN) was placed around the microscope and stage and nitrogen was blown through the tent to minimize oxygen diffusion to the tissue. The microelectrode was reinserted into the suffusion medium and stepped through the medium until it reached the tumor surface.

The microelectrode was placed into an extravascular region, ≥50 μm below the tissue surface, to minimize perturbations of oxygen gradients between the tissue and the overlying suffusion medium (20). For the next 60 to 80 minutes, pO_2 values were continuously recorded. Simultaneously, 1-minute videotape segments of the microvessels containing circulating fluorescently labeled red cells and liposomes were made every 5 minutes. Light was turned off between measurements to minimize photobleaching.

At the end of each experiment, animals were euthanized, leaving the oxygen electrode in place. The current dropped to a value equivalent to zero pO_2 by 10 minutes after death. This value was used as the *in vivo* zero value as previously described (13). The pO_2 values observed during each experiment were derived from the *in vivo* calibration data as previously described (12, 13, 16, 21). After each experiment, the radial distance from the measurement point to each microvessel was determined from the tracings of the vessels, with calibration from a stage micrometer.

Fluorescent red cell fluxes were determined by counting the number of fluorescently labeled cells that passed a preset position near the middle of each vessel segment (midpoint between branch points) over 1-minute intervals (16). Total red cell flux was determined by dividing the number of counted fluorescent cells by the labeled fraction as determined by flow cytometric analysis of a peripheral blood sample obtained after the fluorescently labeled red cells were administered. Two samples were obtained in each experiment, one just after the cells were administered and the second at the end of the experiment. These values did not change appreciably during the experiments, indicating that systemic levels of circulating fluorescently labeled red cells were stable over the period of observation (data not shown).

Results

Eight successful experiments were conducted. Another seven were not completed because of anesthetic deaths (n = 2) or technical complications (n = 5). Aside from the two anesthetic deaths, animals maintained a stable level of anesthesia throughout these experiments. Blood pressures and heart rates averaged 109 ± 8.3 mm Hg and 389 ± 25 bpm, respectively, and were stable over

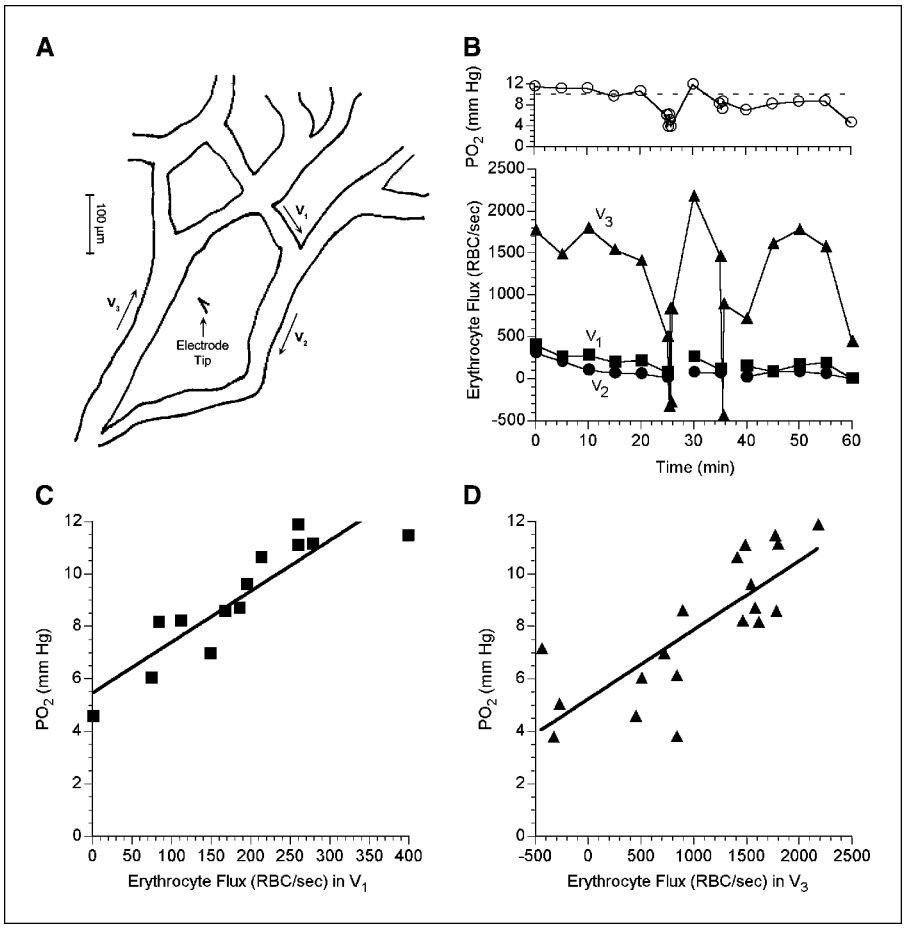

Figure 1. Results from experiment 8 during a 60-minute period of observation. *A,* tracing of microvascular network and position of microelectrode. *B,* interstitial pO_2 and red cell flux for vessel segments 1 to 3. Note negative values for vessel 3 (*V3*), indicating flow reversal. *C,* relationship between tissue pO_2 and red cell flux in vessel 1 (*V1*). The regression line is described as $pO_2 = 0.0194 \times RCF + 5.45$ ($r^2 = 0.809$, $n = 13$, $P < 0.001$). *D,* relationship between tissue pO_2 and red cell flux in vessel 3 (*V3*). The flow reversal data are shown as negative red cell flux values on the plot. The regression line is described as $pO_2 = -0.0026 \times RCF + 5.22$ ($r^2 = 0.624$, $n = 19$, $P < 0.001$).

Downloaded from cancerres.aacrjournals.org on September 20, 2020. © 2006 American Association for Cancer Research.

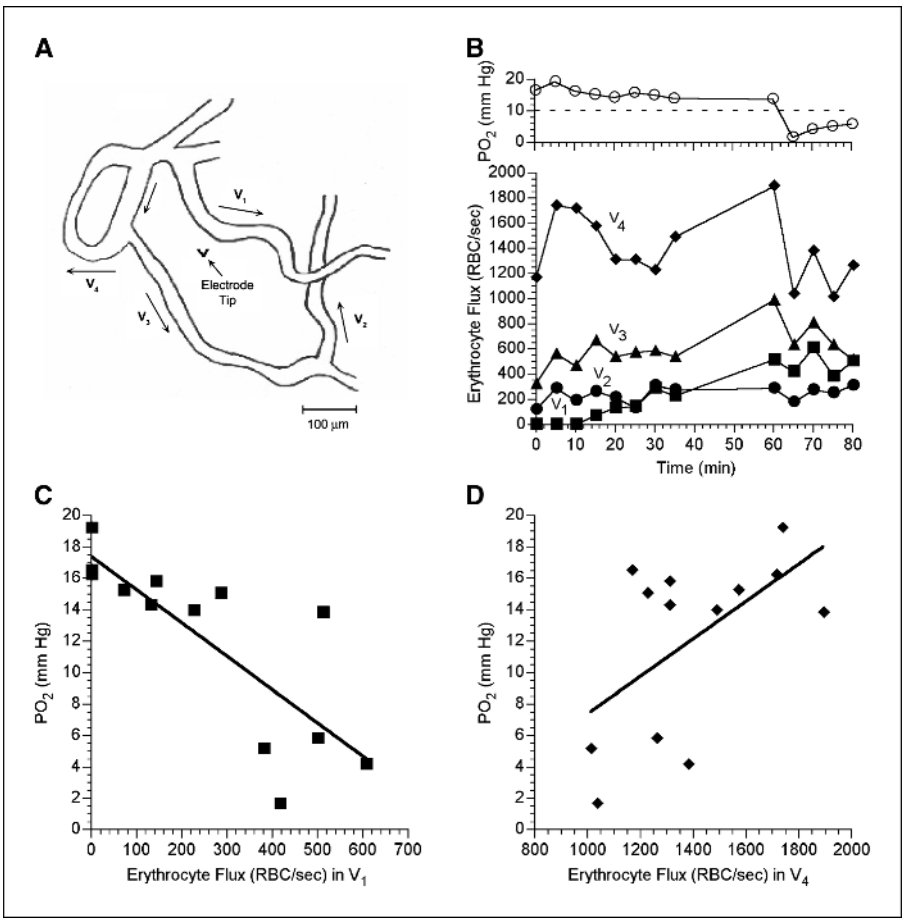

Figure 2. Results from experiment 5 during an 80-minute period of observation. *A,* tracing of microvascular network and position of microelectrode. *B,* interstitial pO_2 and red cell flux for vessel segments 1 to 4. *C,* relationship between tissue pO_2 and red cell flux in vessel 1. The regression line is described as $pO_2 = -0.021 \times RCF + 17.4$ ($r^2 = 0.635$, $n = 13$, $P = 0.001$). *D,* relationship between tissue pO_2 and red cell flux in vessel 4. The regression line is described as $pO_2 = 0.012 \times RCF + 4.56$ ($r^2 = 0.327$, $n = 13$, $P = 0.04$).

the time of measurement (data not shown). These values are well within limits for awake, unanesthetized rats of this strain (22) and are typical for this anesthetic regimen in our prior experience (12, 16, 21).

Examples of results are shown in Figs. 1 and 2. In the first example, a network of three vessels was identified (Fig. 1*A*). One of the vessels (V3) carried a much larger red cell flux than the other two (Fig. 1*B*). During the period of observation, this microvessel exhibited two brief periods of flow reversal, at 25 and 35 minutes. Effects on interstitial pO_2 value were discernable, particularly at 25 minutes (Fig. 1*B*). The influence of red cell flux on interstitial pO_2 can be examined by removing the time factor and plotting pO_2 as a function of red cell flux (Fig. 1*C* and *D*). The relationship between the two was linear when comparing data for each vessel alone (Fig. 1*C* and *D*) and for total red cell flux (flux added together for all three microvessels; data not shown).

In the second example, a network of four vessels was examined (Fig. 2*A*). Again, pO_2 and red cell flux were temporally unstable (Fig. 2*B*). The relationship between pO_2 and red cell flux was complex, indicating a mixture of relatively oxygenated and deoxygenated blood entering this network. The relationship between red cell flux and pO_2 showed a positive slope for vessel 1 (V1, Fig. 2*C*), a negative slope for vessel 4 (V4, Fig. 2*D*), and no detectable relationship for vessels 2 and 3 (data not shown). There was no significant relationship between total red cell flux and pO_2 in this case (data not shown; $r^2 = 0.02$).

In all experiments, pO_2 was temporally unstable (Fig. 3). However, the degree of fluctuation varied from one experiment to another. To examine whether the magnitude of the fluctuations was influenced by proximity to the vasculature, we plotted the median pO_2 and range as a function of distance from the microvessel in the network with the highest red cell flux (Fig. 4). The vessel with the highest red cell flux would be expected to have the greatest influence on tissue pO_2 in such circumstances, as this vessel would have the greatest oxygen carrying capacity. Figure 4 includes variations in perivascular pO_2 (measurements made on the outer wall of microvessels) obtained from a prior publication using the same tumor model (16). Neither the median nor the range of the fluctuations seemed to be predictably influenced by radial distance. However, it is noteworthy that in experiment 7, the distance from the vessel was maximal (140 μm) and pO_2 variations in the range below 5 mm Hg were observed (Fig. 3).

Discussion

This study confirms our previous theoretical prediction (16) that fluctuations in red cell flux lead to temporal variations in extravascular pO_2 ranging up to the diffusion distance of oxygen. These variations in pO_2 are superimposed on the decline in pO_2 with distance from the nearest microvessel (Fig. 4). The results are consistent with prior work indicating that fluctuation in red cell flux in tumor microvessels is common and that this leads to changes in extravascular pO_2 that are of potential radiobiological importance. In other studies using tumors growing in animal flanks, we observed similar kinetics of pO_2 fluctuation (23).

Downloaded from cancerres.aacrjournals.org on September 20, 2020. © 2006 American Association for Cancer Research.

In these experiments, steady-state chronic hypoxia was not observed even at the limit of the oxygen diffusion distance. Experiment 7 showed a condition of chronic hypoxia at a point 140 μm from the vessel with highest red cell flux but fluctuations of ±2 mm Hg were observed in that case as well. In one case (Fig. 2*D*), pO_2 showed a negative correlation with red cell flux in a particular vessel, suggesting that the vessel was acting as an oxygen sink by supplying deoxygenated blood. We have recently identified anastomoses between hypoxic and more aerobic vessels in a mouse mammary carcinoma line, grown in skin-fold window chambers, using hyperspectral imaging to measure hemoglobin saturation in vascular networks (24). These hypoxic vessels were emerging onto the tumor surface from the underlying tumor and presumably were deoxygenated because they had traversed through the tumor before reaching the surface that we were visualizing. We observed these vessels to be consistently hypoxic over several days of observation. It is likely that the diametrically opposed relationship between pO_2 and red cell flux in two different vessels of the same network, as depicted in Fig. 2, was due to a similar vascular arrangement.

The mechanisms underlying the observed variations in red cell flux remain to be determined. Potential mechanisms include arterial vasomotion (25) or vascular remodeling occurring concomitantly with angiogenesis (26). Studies using the dye mismatch method, which reflects variations in perfusion (but does not directly indicate oxygenation), suggest that the variations typically involve groups of vessels as opposed to single isolated vessels (7, 27), consistent with our previous findings (16).

The presence of intermittent hypoxia has several implications with respect to tumor biology and therapy. Genetic instability may arise as a result of free radicals generated during hypoxia-reoxygenation injury (28) and/or as a result of reduced capacity to repair DNA damage (29). Intermittent blood flow and oxygenation may contribute to drug resistance (7). Hypoxia-mediated cytotoxins are being developed to

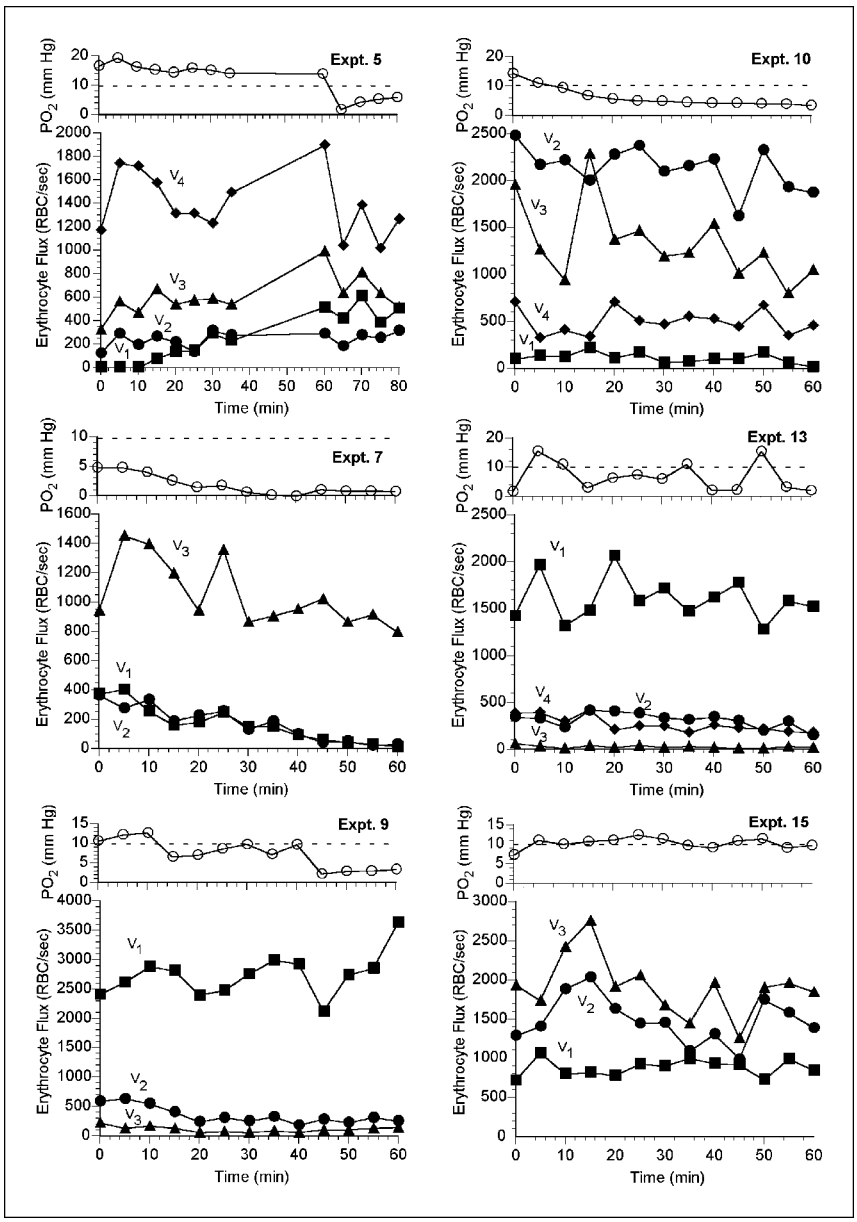

Figure 3. Temporal measurement of pO_2 in all experiments. *Dashed line,* 10 mm Hg threshold. With one exception (experiment 7), pO_2 values fluctuated across the 10 mm Hg boundary at least once during the period of observation.

Downloaded from cancerres.aacrjournals.org on September 20, 2020. © 2006 American Association for Cancer Research.

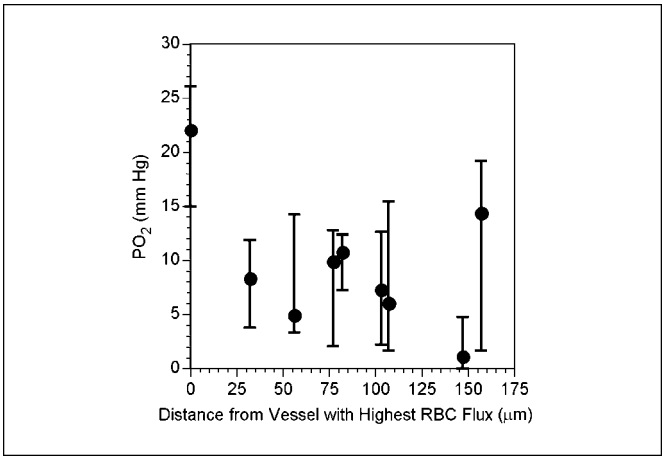

Figure 4. Median (range) of pO_2 values as function of radial distance from the microvessel with the highest red cell flux. Each data point represents one experiment. Data at zero distance are derived from a prior publication in which perivascular pO_2 was measured as a function of time (17). The perivascular pO_2 data indicate the average median, minimum, and maximum of 10 experiments.

target cells that escape radiation treatment in hypoxic regions (30). Fluctuations in tissue oxygenation may compromise the effectiveness of this approach if regions of tumor are not hypoxic during the time of drug exposure. Recently, our group has shown that reoxygenation postirradiation can cause up-regulation of hypoxia inducible factor 1–mediated gene transcription (31).

The prevalence of fluctuating hypoxia in human tumors is unknown. Its characteristics in preclinical models may depend on tumor type (32). Recently, we compared the kinetics of pO_2 fluctuations in three rat tumor lines: the R3230Ac mammary tumor, the 9L glioma, and a fibrosarcoma (33, 34). The dominant frequencies were low, <0.3 cycles per minute, for all three tumor types but amplitudes varied widely. Similar results have been reported for early passage human melanoma xenografts (35, 36). Fluctuations in red cell flux have been measured using laser Doppler flowmetry in several human tumor xenograft lines and in human tumors (37–39). It remains to be determined whether fluctuations in pO_2 are present and lead to radiobiologically significant fluctuations in tumor hypoxia in human subjects.

Acknowledgments

Received 9/18/2005; revised 11/3/2005; accepted 12/14/2005.

Grant support: NIH/National Cancer Institute grant CA40355.

The costs of publication of this article were defrayed in part by the payment of page charges. This article must therefore be hereby marked *advertisement* in accordance with 18 U.S.C. Section 1734 solely to indicate this fact.

We thank Dr. Rachel Richardson for her support in the preparation of this manuscript.

References

1. Coleman CN. Hypoxia in tumors: a paradigm for the approach to biochemical and physiologic heterogeneity. J Natl Cancer Inst 1988;80:310–7.
2. Horsman MR, Overgaard J, Christensen KL, Trotter MJ, Chaplin DJ. Mechanism for the reduction of tumour hypoxia by nicotinamide and the clinical relevance for radiotherapy. Biomed Biochim Acta 1989;48:S251–4.
3. Knowles HJ, Harris AL. Hypoxia and oxidative stress in breast cancer. Hypoxia and tumourigenesis. Breast Cancer Res 2001;3:318–22.
4. Brown JM, Giaccia AJ. The unique physiology of solid tumors: opportunities (and problems) for cancer therapy. Cancer Res 1998;58:1408–16.
5. Dewhirst MW. Concepts of oxygen transport at the microcirculatory level. Semin Radiat Oncol 1998;8:143–50.
6. Durand R, LePard N. Contribution of transient blood flow to tumour hypoxia in mice. Acta Oncol 1995;34:57–61.
7. Durand RE. Intermittent blood flow in solid tumours—an under-appreciated source of "drug resistance." Cancer Metastasis Rev 2001;20:57–61.
8. Secomb T, Hsu R, Braun R, Ross J, Gross J, Dewhirst M. Analysis of oxygen transport to tumors: causes of heterogeneous tissue oxygenation. In: 1999 Bioengineering Conference; 1999. p. 487–88.
9. Secomb TW, Hsu R, Braun RD, Ross JR, Gross JF, Dewhirst MW. Theoretical simulation of oxygen transport to tumors by three-dimensional networks of microvessels. Adv Exp Med Biol 1998;454:313–6.
10. Secomb TW, Hsu R, Ong ET, Gross JF, Dewhirst MW. Analysis of the effects of oxygen supply and demand on hypoxic fraction in tumors. Acta Oncol 1995;34:313–6.
11. Dewhirst M. Angiogenesis and blood flow in solid tumors. In: Teicher BA, editor. Drug resistance in oncology. New York: Marcel Dekker, Inc.; 1993. p. 3–24.
12. Dewhirst M, Ong E, Rosner G, et al. Arteriolar oxygenation in tumor and subcutaneous arterioles: effects of inspired air oxygen content. Br J Cancer 1996; 74:171–82.
13. Dewhirst MW, Ong ET, Klitzman B, et al. Perivascular oxygen tensions in a transplantable mammary tumor growing in a dorsal flap window chamber. Radiat Res 1992;130:171–82.
14. Dewhirst MW, Ong ET, Braun RD, et al. Quantification of longitudinal tissue pO_2 gradients in window chamber tumours: impact on tumour hypoxia. Br J Cancer 1999;79:1717–22.
15. Helmlinger G, Yuan F, Dellian M, Jain R. Interstitial pH and pO_2 gradients in solid tumors *in vivo*: high resolution measurements reveal a lack of correlation. Nat Med 1997;3:5522–8.
16. Kimura H, Braun RD, Ong ET, et al. Fluctuations in red cell flux in tumor microvessels can lead to transient hypoxia and reoxygenation in tumor parenchyma. Cancer Res 1996;56:5522–8.
17. Papenfuss D, Gross J, Intaglietta M, Treese F. A transparent access chamber for the rat dorsal skin fold. Microvasc Res 1979;18:723–6.
18. Linsenmeier R, Yancey C. Improved fabrication of double-barreled recessed cathode oxygen microelectrodes. J Appl Physiol 1987;63:2554–7.
19. Unthank J, Lash J, Nixon J, Sidner R, Bohlen H. Evaluation of carbocyaninelabeled erythrocytes for microvascular measurements. Microvasc Res 1993;45: 193–210.
20. Klitzman B, Popel A, Duling B. Oxygen transport in resting and contracting hamster cremaster muscles: experimental and theoretical microvascular studies. Microvasc Res 1983;25:108–31.
21. Dewhirst MW, Braun RD, Lanzen JL. Temporal changes in pO_2 of R3230AC tumors in Fischer-344 rats. Int J Radiat Oncol Biol Phys 1998;42:723–6.
22. Smith T, Osborne S, Hutchins P. Longterm micro- and macrocirculatory measurements in conscious rats. Microvasc Res 1985;29:260–72.
23. Braun R, Lanzen J, Dewhirst M. Fourier analysis of fluctuations of oxygen tension and blood flow in R3230Ac tumors and muscle of rats. Am J Physiol 1999;277:H551–68.
24. Sorg B, Moeller B, Donovan O, Cao Y, Dewhirst M. Hyperspectral imaging of hemoglobin saturation in tumor microvasculature and tumor hypoxia development. J Biomed Opt 2005;74:S247044004-044001–11.
25. Dewhirst M, Kimura H, Rehmus S, et al. Microvascular studies on the origins of perfusion-limited hypoxia. Br J Cancer 1996;74:S247–51.
26. Patan S, Munn LL, Jain RK. Intussusceptive microvascular growth in a human colon adenocarcinoma xenograft: a novel mechanism of tumor angiogenesis. Microvasc Res 1996;51:260–72.
27. Durand RE, Aquino-Parsons C. Clinical relevance of intermittent tumour blood flow. Acta Oncol 2001;40:929–36.
28. Reynolds TY, Rockwell S, Glazer PM. Genetic instability induced by the tumor microenvironment. Cancer Res 1996;56:5754–7.
29. Mihaylova VT, Bindra RS, Yuan J, et al. Decreased expression of the DNA mismatch repair gene Mlh1 under hypoxic stress in mammalian cells. Mol Cell Biol 2003;23:3265–73.
30. Hicks KO, Siim BG, Pruijn FB, Wilson WR. Oxygen dependence of the metabolic activation and cytotoxicity of tirapazamine: implications for extravascular transport and activity in tumors. Radiat Res 2004;161:656–66.
31. Moeller BJ, Cao Y, Li CY, Dewhirst MW. Radiation activates HIF-1 to regulate vascular radiosensitivity in tumors: role of reoxygenation, free radicals, and stress granules. Cancer Cell 2004;5:429–41.
32. Bennewith KL, Durand RE. Drug-induced alterations in tumour perfusion yield increases in tumour cell radiosensitivity. Br J Cancer 2001;85:1577–84.
33. Cardenas-Navia LI, Braun R, Lewis K, Dewhirst M. Comparison of fluctuations of oxygen tension in FSA, 9L, R3230AC tumors in rats. Adv Exp Med Biol 2003; 510:6010–7.
34. Cardenas-Navia LI, Yu D, Braun RD, Brizel DM, Secomb TW, Dewhirst MW. Tumor-dependent kinetics of partial pressure of oxygen fluctuations during air and oxygen breathing. Cancer Res 2004;64:6010–7.
35. Brurberg KG, Graff BA, Olsen DR, Rofstad EK. Tumor-line specific pO(2) fluctuations in human melanoma xenografts. Int J Radiat Oncol Biol Phys 2004;58:403–9.
36. Brurberg KG, Graff BA, Rofstad EK. Temporal heterogeneity in oxygen tension in human melanoma xenografts. Br J Cancer 2003;89:350–6.
37. Hill S, Pigott K, Saunders M, et al. Microregional blood flow in murine and human tumours assessed using laser Doppler microprobes. Br J Cancer 1996;74: 45–50.
38. Pigott KH, Hill SA, Chaplin DJ, Saunders MI. Microregional fluctuations in perfusion within human tumours detected using laser Doppler flowmetry. Radiother Oncol 1996;40:45–50.
39. Chaplin D, Hill S. Temporal heterogeneity in microregional erythrocyte flux in experimental solid tumours. Br J Cancer 1995;71:1210–3.

Downloaded from cancerres.aacrjournals.org on September 20, 2020. © 2006 American Association for Cancer Research.

AACR American Association for Cancer Research

Cancer Research
The Journal of Cancer Research (1916–1930) | The American Journal of Cancer (1931–1940)

Direct Demonstration of Instabilities in Oxygen Concentrations within the Extravascular Compartment of an Experimental Tumor

Jennifer Lanzen, Rod D. Braun, Bruce Klitzman, et al.

Cancer Res 2006;66:2219-2223.

Updated version	Access the most recent version of this article at: http://cancerres.aacrjournals.org/content/66/4/2219

Cited articles	This article cites 35 articles, 5 of which you can access for free at: http://cancerres.aacrjournals.org/content/66/4/2219.full#ref-list-1
Citing articles	This article has been cited by 23 HighWire-hosted articles. Access the articles at: http://cancerres.aacrjournals.org/content/66/4/2219.full#related-urls

E-mail alerts	Sign up to receive free email-alerts related to this article or journal.
Reprints and Subscriptions	To order reprints of this article or to subscribe to the journal, contact the AACR Publications Department at pubs@aacr.org.
Permissions	To request permission to re-use all or part of this article, use this link http://cancerres.aacrjournals.org/content/66/4/2219. Click on "Request Permissions" which will take you to the Copyright Clearance Center's (CCC) Rightslink site.

Downloaded from cancerres.aacrjournals.org on September 20, 2020. © 2006 American Association for Cancer Research.